ELSEVIER

Thin Solid Films 281–282 (1996) 256–259

thin solid films

Diamond (111) and (100) surface reconstructions

A. Scholze *, W.G. Schmidt, F. Bechstedt

Friedrich-Schiller-Universität, Institut für Festkörpertheorie und Theoretische Optik, Max-Wien-Platz 1, 07743 Jena, Germany

---

Abstract

Fully converged ab initio density functional theory local density approximation (DFT-LDA) calculations are presented for C(111) and C(100) surfaces using soft carbon pseudopotentials and plane waves with a cutoff energy of 42 Ry. For the single and triple dangling bond surfaces, we study 2 × 1 and ($\sqrt{3}\times\sqrt{3}$)R30° reconstructions with respect to their total energies, geometries and band structures. In contrast with an earlier ab initio study, we find that the π-bonded chains are not dimerized in the 2 × 1 Pandey reconstruction. Chain and trimer reconstructions of the triple dangling bond face result in a considerable lowering of the total energy. The ground state of the (100) face is governed by symmetric dimers resulting in a 2 × 1 reconstruction.

Keywords: Density functional calculations; Diamond; Low-index single-crystal surfaces; Molecular dynamics; Surface relaxation and reconstruction

---

1. Introduction

Due to its extreme properties, diamond has become a very interesting material for various applications in the last decade. Much of this interest is drawn to the low-index planes of diamond because of their importance in thin film growth by chemical vapour deposition (CVD). For both homoepitaxial and heteroepitaxial growth, as well as for the fabrication of diamond–silicon or diamond–metal interfaces, an accurate understanding of the low-index faces of diamond is vital. However, despite long-standing activities in this field, the atomic and electronic structures of C(111) and C(100) surfaces are not completely understood. In the case of C(111)2 × 1, details such as the dimerization or buckling of the energetically favoured π-bonded chains remain to be clarified [1,2]. Moreover, the role of the triple dangling bond (TDB) (glide plane) cleavage face vs. that of the single dangling bond (SDB) (shuffle plane) cleavage face is still unclear [3]. The experimentally observed surface state gap [4] can be theoretically reproduced only by taking significant chain dimerization into account [5]. However, such dimerization leads to an energy loss related to subsurface strains [6]. Recent scanning tunnelling microscopy (STM) measurements [7] provide some evidence for a ($\sqrt{3}\times\sqrt{3}$)R30° surface reconstruction on the (111) faces of polycrystalline films grown by CVD.

The dimer reconstruction of the clean C(100)2 × 1 surface is now well established [8–10]. However, the possibility of higher reconstructions, as in the silicon case, is an open problem, as are details of the band structure resulting from the dimer reconstruction.

In this paper, we present first principles total energy calculations to determine the atomic structure and electronic properties of C(111) and C(100) surfaces with different reconstructions.

2. Method

Our calculations are based on the density functional theory (DFT) and the local density approximation (LDA) [11]. The single-particle wavefunctions are expanded into plane waves. The electron–ion interaction is treated by norm-conserving, ab initio, fully separable pseudopotentials. After softening the carbon pseudopotential [12], the energy cutoff can be restricted to 42 Ry. For bulk diamond, this procedure gives rise to a lattice constant of 3.534 Å, being 0.9% smaller than the experimental value (3.567 Å). The experimental values of the bulk modulus (4.42 Mbar) and the TO(Γ) phonon frequency (250.7 THz) are well reproduced at 4.56 Mbar and 245.1 THz respectively. However, the DFT-LDA value for the indirect gap of 4.09 eV underestimates the experimental value (5.5 eV) by about 25%. We use the repeated slab method to simulate the surfaces. The 2 × 1 and ($\sqrt{3}\times\sqrt{3}$)R30° reconstructions are represented by symmetric slabs of 12 or 10 atomic layers of carbon and a vacuum region

---

* Corresponding author. Fax: +49 3641 635 182; e-mail: andreas@ifto.physik.uni-jena.de.

PII S0040-6090(96)08646-4

equivalent in thickness. Hydrogen terminated slabs are used to calculate 2×2 reconstructions. The **k** space integration is replaced by a summation over four (one) special points in the irreducible part of the two-dimensional surface Brillouin zone (SBZ) for the rectangular (hexagonal) case. In order to determine the equilibrium positions, the atoms of the two innermost substrate layers are kept frozen, whereas all other atoms are allowed to relax until the total energy and the forces on the atoms are minimized. Simultaneously, the single-particle wavefunctions are brought to self-consistency within a Car–Parrinello-like minimization scheme of the total energy functional [11]. The reconstruction energy E_{rec} is derived with respect to the ideal bulk terminated surface. The surface energy E_{sur} is the sum of half the energy per 1×1 unit cell which is needed to cleave the ideal crystal and the reconstruction energy.

Table 1
Reconstruction energy (E_{rec}) and surface formation energy per 1×1 unit cell (E_{sur}) for stable and metastable energy minimum structures

Surface	Reconstruction	E_{rec} (eV)	E_{sur} (eV)
C(111)1×1 SDB	Bulk terminated	0.00	3.27
	Relaxed bulk terminated	−0.57	2.70
C(111)2×1 SDB	Chadi π-bonded molecule	−0.73	2.54
	Pandey π-bonded chain	−1.40	1.87
C(111)1×1 TDB	Bulk terminated	0.00	5.15
C(111)2×1 TDB	Seiwatz single chains	−1.93	3.22
C(111)(√3×√3)-R30° TDB	H-site trimer	−1.73	3.42
C(100)2×1	Bulk terminated	0.00	4.88
	Symmetric dimer	−1.61	3.27

3. Results

The as-polished C(111) surface has been found to undergo a transition from a 1×1 to a 2×2 low-energy electron diffraction (LEED) pattern on annealing [13,14]. Usually the resulting structure is interpreted as a superposition of three twisted 2×1 domains of SDB cleavage faces which exhibit a π-bonded chain structure [1]. We confirm this result. In agreement with other calculations [1,2,15], we find the lowest energy for the chain model (Fig. 1(a)). The energy gain of 1.4 eV per 1×1 unit cell is much larger than that for the other structures (cf. Table 1), e.g. the relaxed surface or Chadi π-bonded molecule model (Fig. 1(b)). In our calculations, a graphitic-like surface reconstruction recently discussed as a metastable state [16] on the (111) face is found to give only a saddle point on the total energy surface. The geometrical details of the resulting π-bonded chains are consistent with other ab initio calculations [1,2,15]. This also holds for the average chain bond length of 1.43 Å. In agreement with the results of Vanderbilt and Louie [1], our chains remain undimerized and unbuckled considering the accuracy related to the numerical conditions for vanishing Hellmann–Feynman forces. Dimerization of the chains always tends to lead to an increase in the total energy. However, we end up with a small dimerization of about 1% if no point group symmetry is assumed for the surface, but the **k** space summation in the atomic force calculation is restricted to the irreducible part of the BZ.

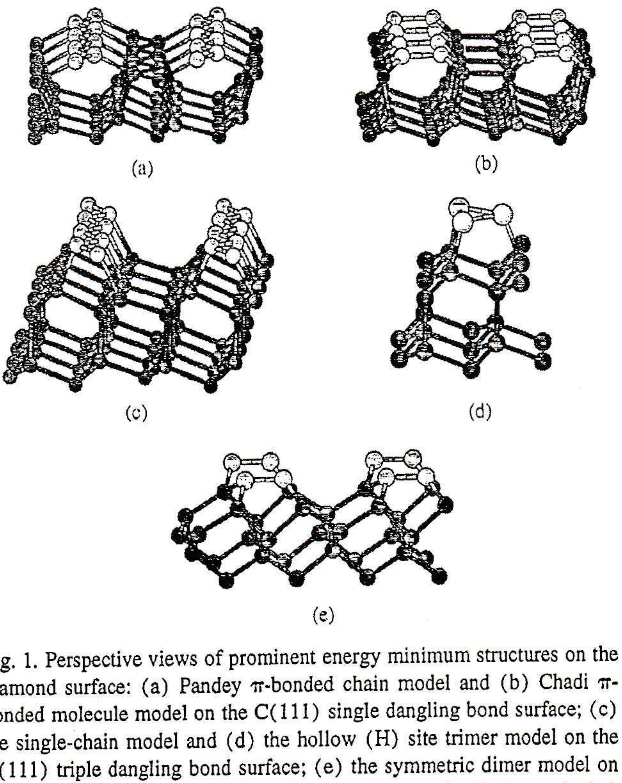

Fig. 1. Perspective views of prominent energy minimum structures on the diamond surface: (a) Pandey π-bonded chain model and (b) Chadi π-bonded molecule model on the C(111) single dangling bond surface; (c) the single-chain model and (d) the hollow (H) site trimer model on the C(111) triple dangling bond surface; (e) the symmetric dimer model on the C(100) surface. Carbon atoms in the uppermost surface layer are shaded.

Fig. 2(a) shows the surface electronic structure of the optimized π-bonded chain geometry. The dominating features in the gap are the mainly occupied (S_2) and unoccupied (S_1) surface bands derived from the π bonding or antibonding combinations of the p orbitals along the chain and perpendicular to the surface. The almost one-dimensional character of the chains is clearly seen from the nearly flat and degenerate bands along J–K which cross the Fermi level and consequently cause a metallic character of the surface within the DFT-LDA approach. The remaining upwards dispersion and the splitting of 0.1 eV at K are due to a weak interchain interaction. Other bands in the gap are associated with bulk states due to the lengthened backbonds. The occupied surface state (S_2) becomes resonant at half the distance Γ–J, lying 1 eV below the valence band maximum (VBM) of the projected bulk band structure and shows an upwards dispersion towards J. This is in reasonable agreement with angle-resolved photoemission spectroscopy (ARPES) data [17]. The splitting of S_1 and S_2 and the position of the unoccupied state at Γ (4.8 eV) are in good agreement with the findings of previous ab initio work [1,2] and the two-photon photoemission (PES) measurements of Kubiak and Kolasinski [18]. However, the latter agreement may be somewhat fortuitous because of the general underestimation of one-electron excitation energies in DFT-LDA calculations. Kress et

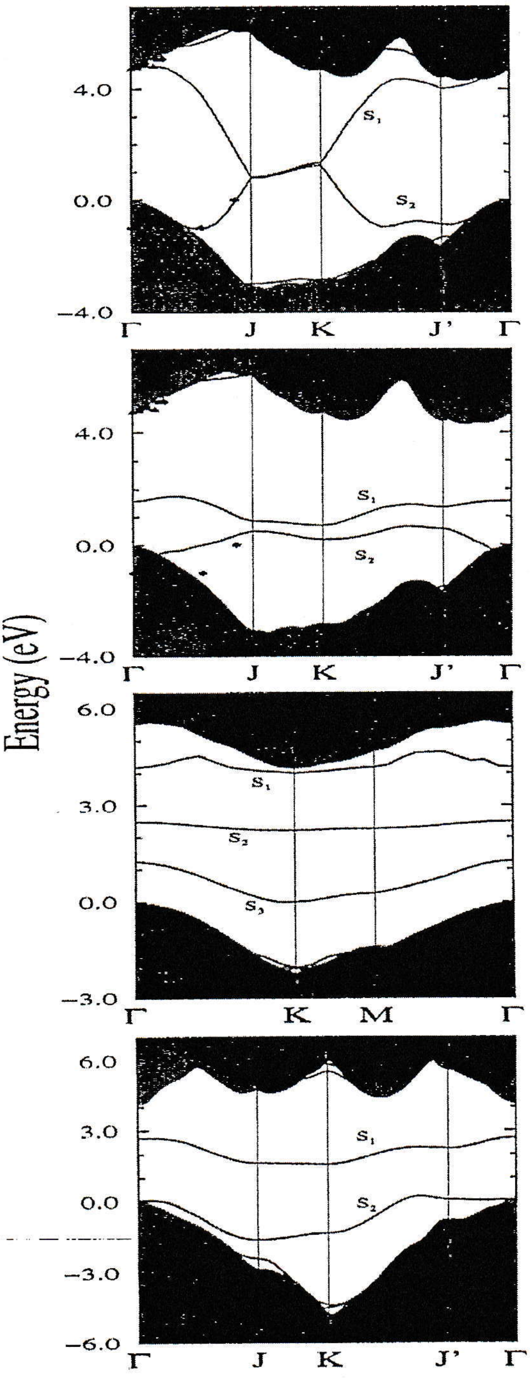

Fig. 2. Surface bands and projected bulk band structure (shaded) for several diamond surfaces. Experimental data from photoemission (PES) are shown for comparison: ◆, [17]; ▲, [18]. (a) C(111)2×1 SDB, Pandey π-bonded chain structure; (b) C(111)2×1 TDB, Seiwatz single-chain structure; (c) C(111)($\sqrt{3}\times\sqrt{3}$)R30° TDB, H-site trimeric structure; (d) C(100)2×1, symmetric dimer structure.

al. [8] calculated an upwards shift of the unoccupied states and a conduction band minimum (CBM) of the projected bulk band structure of more than 1 eV at Γ applying a quasiparticle (GW) formalism. They showed that the degeneracy of the bands along J–K would be lifted if the chains were dimerized. The degeneracy of the two surface states along J–K disagrees with the surface energy gap seemingly observed within electron energy loss spectroscopy (EELS) [19]. However, other solutions of this puzzle are possible. When the single-quasiparticle equations are solved directly, a surface state gap at J and K is conceivable also within the undimerized π-bonded chain model. On the other hand, more complex reconstructions cannot be excluded completely.

In the case of silicon, reconstructions based on TDB (glide plane) cleavage have been shown to match several experimental data [3], although this cleavage should be unfavourable from the energetic point of view. Moreover, Zheng and Smith [20] suggested that hydrogen plays an important role in the diamond cleavage process, so that the TDB surface can provide the energetically favourable configuration. Experiments have shown that hydrogen is always present on bulk diamond and CVD layers [13]. Huang et al. [21] suggest that dislocations at glide planes could be a natural explanation for TDB cleavage. Consequently, in addition to the SDB surface, we discuss results for the TDB surface. Recent STM results [7] have shown that ($\sqrt{3}\times\sqrt{3}$)R30° structures may coexist with conventional 2×1 structures. Apart from adatom models, reconstructions in ($\sqrt{3}\times\sqrt{3}$)R30° unit cells are difficult to imagine at the SDB surface. However, on the TDB surface, such reconstructions can occur quite naturally.

The ($\sqrt{3}\times\sqrt{3}$)R30° reconstruction is thought to consist of trimeric structures that are centred at a hollow (H) site position on the TDB surface [7]. This structure is shown in Fig. 1(d). The atoms forming the trimer are bonded with one bond to a carbon atom in the top substrate layer. The other bonds participate in strong trimer bonding. The energy gain on relaxation is 1.73 eV. The equilibrium bond length of the two shorter bonds is 1.39 Å. The angle between these bonds is 67°. The electronic band structure is shown in Fig. 2(c).

An earlier model which considers reconstruction on the TDB surface is the Seiwatz single-chain structure (Fig. 1(c)). This reconstruction takes place in a 2×1 unit cell. It is characterized by the formation of isolated zig-zag chains with a bonding of the chain atoms similar to the Pandey chain model. However, the π bonding on the surface is not as strong as in the Pandey chain model. Consequently, the bond length in the chain is, at 1.45 Å, slightly larger. This is due to the fact that, in the Seiwatz model, the p orbitals are more inclined to each other and far from vertical with respect to the surface normal. Dimerization of the chain has not been found. Zheng and Smith [20] found, in principle, the same structure, but a buckling of 0.27 Å, which is five times larger than our result. The reconstruction energy is, at 1.92 eV, very high, exceeding the value for the Pandey chain model by 0.52 eV. The similarity to the reconstruction energy of the trimeric structure (1.73 eV) suggests that both structures may coexist on the C(111) TDB surface. There have been observations of both unit cells on the (111) surface; however, it is rather difficult for STM measurements to distinguish clearly between the Seiwatz structure and the Pandey chain structure since both appear in a 2×1 unit cell [7]. The electronic band structure of the Seiwatz model is in poor agreement with PES data (cf. Fig. 2(b)). The weaker π bonding results in a narrower splitting of the bands.

For the determination of the energy minimum structure for the C(100) surface, we started with different geometries: symmetric and asymmetric 2×1 dimer reconstructions as well as a 2×2 surface reconstruction consisting of two oppositely buckled dimers. All these starting configurations relax to the same 2×1 reconstructed surface which is characterized by symmetric dimers (Fig. 1(e)). This finding is in contrast with the ab initio DFT-LDA results for the Si(100)2×1 surface. Two possible reasons may be mentioned. Firstly, in the case of carbon atoms, there is a tendency to form double bonds even at the surface. The energy gain due to the formation of a strong, completely covalent C=C double bond is larger than that of a weaker partially ionic bond. Secondly, as already indicated for the C(111) surface, e.g. for the almost undimerized and unbuckled Pandey π-bonded chains, asymmetric structures are unfavourable in the diamond case, since they are accompanied by subsurface strains which give rise to a remarkable energy loss due to the stronger carbon bonding. Our results are in agreement with other ab initio calculations [8–10,15]. This holds especially for the dimer bond length of 1.36 Å.

The electronic structure of the symmetrically dimerized C(100)2×1 surface resulting from the optimized geometry is presented in Fig. 2(d). The strong σ and π bonds of the dimers give rise to bands with prominent surface state character. Within the fundamental gap, the bands related to the bonding (π) and antibonding (π^*) combinations of the p orbitals parallel to the surface normal are dominant. This is somewhat in contrast with the Si case, where the character of the states forming the two bands is defined more by dangling bonds at the lower and upper atoms in the buckled dimer. The dispersion of the two bands is weak, thus indicating the isolation of the dimers. The occupied π band is resonant with the bulk valence bands, whereas the π^* band is located near a midgap position. Taking quasiparticle effects into account, the surface gap is opened by about 2 eV [8], whereas the opening of the bulk indirect gap is smaller at 1.6 eV.

4. Conclusions

We have performed DFT-LDA calculations of various atomic configurations for atoms on the C(111) and C(100) surfaces. We found that symmetric π-bonded chains and dimers were the energetically most favourable structural elements. However, in the (111) case, other reconstructions also give rise to local minima in the Born–Oppenheimer total energy surface. This holds especially for the TDB (111) surface, the formation energy of which is much larger than that for the SDB face. However, the energy gains due to reconstructions are also higher. Consequently, we predict the appearance of such C(111) surfaces as long as they do not result from direct cleavage.

Acknowledgements

We acknowledge J. Furthmüller, P. Käckell, J. Pollmann and M. Scheffler for helpful discussions. This work was supported by the Deutsche Forschungsgemeinschaft (project no. Be1346/6-1) and the EC Programme Human Capital and Mobility (contract no. ERBCHRXCT 930 337).

References

[1] D. Vanderbilt and S. Louie, *Phys. Rev. B, 29* (1984) 7099; *30* (1984) 6118.

[2] S. Iarlori, G. Galli, F. Gygi, M. Parinello and E. Tosatti, *Phys. Rev. B, 69* (1992) 2947.

[3] D. Chen and D. Hanemann, *Phys. Rev. B, 51* (1995) 4258.

[4] B.B. Pate, *Surf. Sci., 165* (1986) 83.

[5] C. Kress, M. Fiedler and F. Bechstedt, *Europhys. Lett., 28* (1994) 433.

[6] A. Scholze, W.G. Schmidt, P. Käckell and F. Bechstedt, *Mater. Sci. Eng. B, 37* (1996) 158.

[7] H.G. Busmann, S. Lauer, I.V. Hertel, W. Zimmermann-Edling, H.-J. Güntherodt, Th. Frauenheim, P. Blaudeck and D. Porezag, *Surf. Sci., 295* (1993) 340.

[8] C. Kress, M. Fiedler, W.G. Schmidt and F. Bechstedt, *Phys. Rev. B, 50* (1994) 17 697.

[9] J. Furthmüller, J. Hafner and G. Kresse, *Europhys. Lett., 28* (1994) 659.

[10] P. Krüger and J. Pollmann, *Phys. Rev. Lett., 74* (1994) 1155.

[11] R. Stumpf and M. Scheffler, *Comput. Phys. Commun., 79* (1994) 447.

[12] B. Wenzien, P. Käckell and F. Bechstedt, *Surf. Sci., 307–309* (1994) 989.

[13] A.V. Hamza, G.D. Kubiak and R.H. Stuhlen, *Surf. Sci., 206* (1988) L833.

[14] S.-T. Lee and G. Apai, *Phys. Rev. B, 48* (1994) 2684.

[15] D.R. Alfonso, D.A. Drabold and S.E. Ulloa, *Phys. Rev. B, 51* (1995) 14 669.

[16] G. Jungnickel, A. Porezag, T. Frauenheim, W.R.L. Lambrecht, R. Segall and J.C. Angus, *Symp. Proc. Mater. Res. Soc., 383* (1995) 349.

[17] F.J. Himpsel, D.E. Eastman, P. Heimann and J.F. van der Veen, *Phys. Rev. B, 24* (1981) 7270.

[18] G.D. Kubiak and K.W. Kolasinski, *Phys. Rev. B, 39* (1989) 1381.

[19] S. Pepper, *Surf. Sci., 123* (1982) 47.

[20] X.M. Zheng and P.V. Smith, *Surf. Sci., 253* (1991) 395.

[21] Y.M. Huang, J.C.H. Spence, O.F. Sankey and G.B. Adams, *Surf. Sci., 256* (1991) 344.